08

Sub-THz Range Superconducting SIS Receivers for Space and Ground-Based Radio Astronomy

© K.I. Rudakov,[1,2] F.V. Khan,[1,2,3] L.V. Filippenko,[1,2] A.M. Chekushkin,[1] A.V. Khudchenko,[1,2] V.P. Koshelets[1,2]

[1]Kotelnikov Institute of Radio Engineering and Electronics, Russian Academy of Sciences,
125009 Moscow, Russia
[2]Astro Space Center of P.N. Lebedev Physical Institute of the Russian Academy of Sciences,
117810 Moscow, Russia
[3]Moscow Institute of Physics and Technology (National Research University),
141701 Dolgoprudny, Moscow Region, Russia
e-mail: valery@hitech.cplire.ru

Received May 15, 2024
Revised May 15, 2024
Accepted May 15, 2024

The paper presents the results of developments of low-noise receiving systems in the sub-THz range, carried out at the Kotelnikov Institute of Radio Engineering of the Russian Academy of Sciences in recent years and aimed at creating receivers with quantum sensitivity for use in space and ground-based radio telescopes. The technology for manufacturing integrated receiving structures based on superconductor−insulator−superconductor (SIS) tunnel junctions is described, and the results of the development of SIS receivers in the 211−275 GHz and 800−950 GHz ranges with a noise temperature in double sideband (DSB) mode of about 20 K and 220 K are presented, respectively. The results of these developments will be used to create receiving systems for the ground-based telescopes Suffa, APEX and LLAMA, as well as for the Millimetron space mission.

Keywords: Superconducting devices, superconductor-insulator-superconductor tunnel junction, subTHz range receiving systems .

DOI: 10.61011/TP.2024.07.58805.171-24

Introduction

Development of supersensitive sub-terahertz (THz) receivers is currently one of the most intensively and successfully developed fields of superconducting electronics. Superconducting receiving devices have already proved their excellence in this frequency band [1–5]. Superconducting elements have extremely high characteristic frequency and very strong nonlinearity as well as extremely low intrinsic noise due to quantum nature of the elements and cryogenic operating temperature. Combination of these benefits in a single superconducting element makes it possible to create THz receiving systems with unique parameters that are unavailable to devices with other operating principles. Since the acquisition time for superweak signal receipt and detection of very low substance concentrations is as square of the noise temperature of the utilized devices, superconducting junction receivers can reduce considerably the observation time. Superconducting receivers are currently used worldwide as standard devices on the most ground and space radio telescopes designed to solve fundamental issues of the origin of the Universe. Many applications require spectral resolution $\Delta f/f$ better than 10^{-6}; such resolution may be achieved only using heterodyne receiving systems. A heterodyne mixer converts the incoming weak input signal to a lower intermediate frequency (IF) without phase retardation; the IF signal spectrum is the same as the input one, but is shifted down in frequency to the heterodyne frequency.

Mixers based on superconductor–insulator–superconductor (SIS) tunnel junctions are the most sensitive input devices in heterodyne receivers on frequencies f from 0.1 to 1.2 THz [1,2,5–7]. Under the heterodyne signal, the tunneling current flowing through the junction increases; this process is known as phonon-induced tunneling [1]. The tunneling current may be calculated using a quantum-mechanical model [1,6]. SIS mixers can inherently provide amplified conversion. Low requirements for heterodyne power and very low intrinsic noise are the important advantages of SIS mixers [1,2,6,7]. Double-sideband (DSB) noise temperature of the mixer is limited by the quantum value $hf/(2k_B)$ [{]1,8}, where h andk_B are Planck's and Boltzmann's constants, respectively. SIS mixers have been successfully used for space missions and for ground radio telescopes as well [3,4,9]. This is, in particular, supported by successful observations of the M87 supermassive black hole shadow in the center of galaxy [10,11] in the framework of the EHT (Event Horizon Telescope) project [12] where all measurements were conducted using waveguide SIS mixers with external heterodyne oscillator at a frequency about 230 GHz. SIS mixers employed in radio observatories under the EHT project have shown that the waveguide version of receiver configuration is the most reliable and useful, and provides high stability and sensitivity. A very high angular resolution

will be implemented in the „Millimetron“ project of the Russian Space Agency (RSA) designed to create a space-to-ground radio interferometer with a base of 1.5 mln. kilometers [13,14].

1. SIS tunnel junctions

To implement peak performance of receiving systems, SIS tunnel junctions with extremely low leakage current below the gap voltage V_g and minimized smearing of the energy gap δV_g are necessary. Fabrication process of the Nb−AlO_x−Nb tunnel junctions is based on the fact that a thin Al layer of 5 to 7 nm in thickness can fully cover the base Nb electrode planarizing the columnar microstructure of the Nb film [15,16]. This Al layer is oxidized later and than a top Nb electrode is deposited on the oxidized layer forming a so-called sandwich structure [17,18]. Due to the proximity effect, the Al layer having a long coherency length becomes superconducting forming a Nb/Al−AlO_x/Nb (S−S′/I/S) structure. The presence of Al near the tunneling barrier results in the occurrence of a knee-shaped singularity on the junction CVC at voltages just above V_g. Exact shape of the tunnel junction CVC depend on the density of states of quasiparticles in the S′ layer (Al). This density of states for Nb/Al bilayers was calculated using the microscopic proximity effect model [19]. The model implies a short free electron path (dirty limit conditions) in S (Nb) materials and in S′ (Al) as well. The knee-shaped singularity on CVC results in singularities on quasi-particle steps which in turn results in instability and nonlinearity of mixer performance on some frequencies. To suppress the knee-shape singularity caused by the effect of the normal Al layer, structures with additional Al interlayer in the bottom Nb electrode were proposed [20,21]. And the order parameter in the Nb−Al structure near the barrier becomes spatially-homogeneous and the density of states is close to the distribution used in the Bardeen−Cooper−Schrieffer (BCS) theory making it possible to implement the „ideal“ CVC of the SIS junction (Figure 1).

Formation of SIS tunnel junctions is the essential phase. Minimum repeatable linear dimensions of junctions that may be achieved using the optical photolithography are $0.8\,\mu$m making it possible to create transitions with an area of $0.5\,\mu m^2$. Junctions are formed by reactive ion etching (RIE) in chemically active CF_4 plasma with a typical pressure of$8 \cdot 10^{-2}$ mbar and a power of 50 W by removing the top Nb layer in the multilayer structure using the photoresist mask. An oxidized barrier Al layer is used as the stop layer preventing further etching of the structure. RIE is followed by anodization in ammonia pentaborate ethyleneglycol solution to 10 V using the same masking photoresist, then the H magnetron sputtering method is used to apply the 250 nm SiO_2 layer . Anodization is necessary to provide a more reliable insulation on the SIS junction perimeter to avoid possible micro short circuits between the base electrode and top feed electrode in these areas.

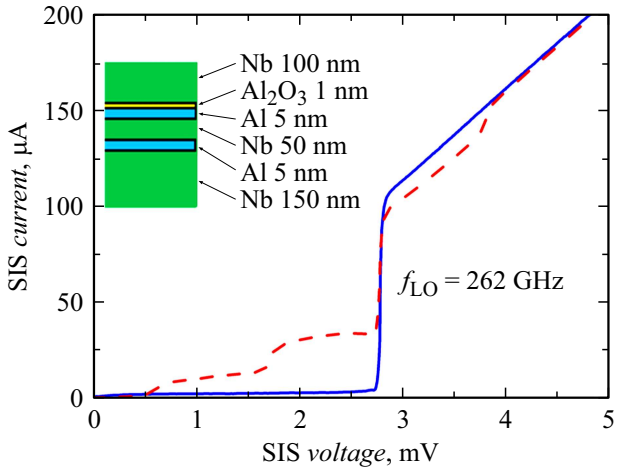

Figure 1. CVC of the Nb−AlO_x−Nb tunnel structure with additional Al interlayer in the bottom Nb electrode (see the detail): the solid blue curve is the offline CVC, dashed line is the CVC with 262 GHz heterodyne signal with the optimum power.

Contacts to the junctions are opened in dimethylformamide by the lift-off lithography method. The top electrode is also formed by the lift-off photolithography from the 350−400 nm Nb layer. Au contact pads for the base and top electrodes are made in the same way.

For operation on frequencies about 1 THz, tunnel junctions with very high transparency of the tunneling barrier are required. There is a AlO_x barrier transparency rise limit (current density about 10−15 kA/cm^2); rapid degradation of the junction occurs at higher current density. This problem was solved by the development of Nb−Al/AlN−Nb tunnel junctions that demonstrate rather good $R_{sg}/R_n > 10$ at very high current densities up to 100 kA/cm^2 [22,23]. The AlN layer is formed by Al nitridation in HF discharge. To achieve good agreement between junctions with such high current density and antenna, submicron SIS junctions, whose geometry is formed by the method described above, are necessary.

The operating frequency of SIS receivers based on Nb films is limited by the Nb energy gap frequency (approx. 700 GHz). This problem can be solved by using microstrip lines made of Nb compounds with higher energy gap frequencies, in particular, NbTiN is used [24–26]; to avoid SIS junction overheating, the top electrode of the line is generally made of metal that remains in normal state at helium temperatures (usually Al). We have developed a SIS mixer consisting of dual Nb/AlN/NbN tunnel junctions with high tunneling current (up to 30 kA/cm^2) built in the microstrip line formed by the 320 nm bottom NbTiN film electrode (grounding plane) and 500 nm top Al electrode [27]. The microstrip line electrodes are separated by the 250 nm SiO_2 insulating layer. The dual SIS junctions are placed on the NbTiN film and are spaced $5-7\,\mu$m apart for capacity offset, and the NbN electrode of the SIS junctions contacts with the top AL electrode of the line. Note that a much

higher energy gap [21] (up to 3.7 mV for junctions with current density up to 10 kA/cm^2 on Si substrate) is another advantage of the Nb−AlN−NbN junctions.

The tunnel structures studied herein were fabricated using the equipment included in the Unique Research Facility „Kriointegral“ — „Technology and Measurement Facility for Fabrication of Superconducting Nanosystems using New Materials“ [28] created by Kotelnikov Institute of Radio Engineering and Electronics RAS. This is a unique facility that is reported to be Russia's only facility where high quality Nb-based tunnel junctions with high current density may be made. Over recent years, a technique of fabrication of Nb−AlO_x−Nb and Nb−AlN−NbN tunnel junctions with high current density and low leakage has been developed [18,20,21,27]. This technique was used to create a multilayer IC technology for IC with the number of elements up to 1 000; the technology was improved to increase the degree of integration and the yield of operating circuits.

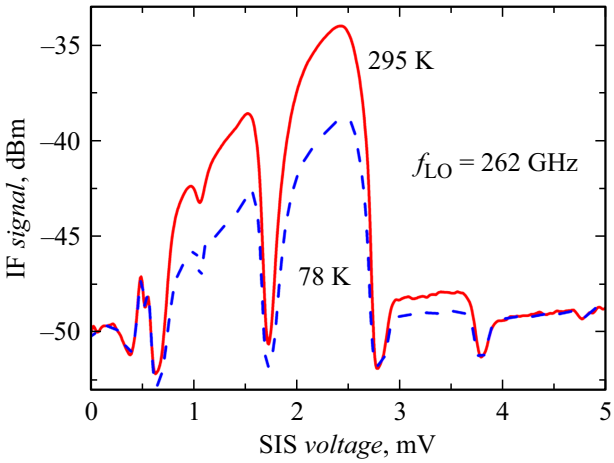

Figure 2. SIS receiver output on IF 6.5 GHz from the bias voltage on SIS measured for cold (78 K — dashed line) and hot (295 K — solid line) input loads at the receiver input at a heterodyne frequency of 262 GHz.

2. Receiving SIS elements and their measurements

To achieve low noise temperature of the SIS receiver, good matching with respect to high (input) and intermediate (output) frequency, low VHF signal loss and high conversion ratio of the mixing element shall be ensured. To estimate the matching bandwidth of the SIS mixer, the Michelson Fourier transform spectrometer (FTS) was used. The sub-THz broadband radiation source (black body heated up to 1500 K) was matched with FTS where a SIS mixer was used as a detector. The voltage on the mixer was set to a value a little lower than the gap voltage; DC response was measured depending on the movable mirror position. The data were used to obtain a matching curve for the mixer with radiation on frequency through the Fourier transform. The experimental data demonstrate good agreement with the numerical simulation in the frequency ranges of 200−300 and 700−950 GHz [21,29].

2.1. 211−275 GHz receiver

Figure 1 shows CVC of the Nb−AlO_x−Nb mixing SIS element exposed to 262 GHz heterodyne signal with the optimum power. When exposed to heterodyne oscillator radiation with frequency f, quasi-particle steps that are away from the gap at hf/e proportional to the heterodyne frequency occur on the offline current-voltage curve (CVC) of the SIS junction. To implement the quasi-particle mixing mode with extremely low noise, the critical current of the SIS junction shall be suppressed by means of a magnetic field set to the tunnel junction. By choosing the operating point on the quasi-particle step of SIS CVC, the best conditions for conversion of the VHF spectrum to IF spectrum may be selected.

To develop the mixer, a mixing element topology was designed, simulation and improvement of the mixing element properties were performed, IC with Nb/AlO_x/Nb tunnel structures with an area about 1 μm^2 were made [21,29]. It is also necessary to compensate the considerable capacity of the SIS junction ($C_{spec} \simeq 0.085$ pF/μm^2) to achieve low noise temperature. As a result, the impedance of the structure decreases to units of Ω and the final impedance of the SIS junction on high frequency shall be matched with the waveguide impedance of about 400 Ω, which was implemented by using a planar structure consisting of Nb/SiO_2/Nb coplanar and microstrip line segments. The receiving element was made on a 125 μm quartz substrate, the mixing element design used HF reject filters to prevent HF signal leakage [21,29]. The receiving element was placed perpendicular to the wave propagation plane in a 500 × 1000 μm rectangular waveguide, 230 μm from the waveguide end to form a quarter-wave short-circuiting jumper. The waveguide chamber (back-peace) includes IC with SIS junction, quarter-wave short-circuiting jumper and IF signal output board to the coaxial connector. The mixing waveguide unit consists of an input horn, central part with waveguide, waveguide chamber and magnetic field setting unit [21,29].

The mixer noise temperature in the double-sideband mode was defined by the standard measurement of Y-factor; a room temperature absorber (295 K) was used as a „hot“ load, and a liquid-nitrogen-cooled absorber (78 K) was used as a „cold“ load. Figure 2 shows the dependence of the SIS receiver output on the bias voltage measured for the 262 GHz heterodyne and IF 6.5 GHz (IF filter bandwidth 60 MHz). Y-factor was calculated by subtracting the IF responses measured in dB for the hot and cold loads. Y-factor in the best point exceeds 5.0 dB, which corresponds to the receiver noise temperature below 20 K.

DSB noise temperatures T_n were obtained without any corrections for beam splitter and cryostat window loss; they were only twice as high as hf/k_B in the frequency range from 240 to 275 GHz; the obtained values correspond to the specifications of the 211–275 GHz receiver of the „Millimetron“ space radio telescope[13,14].

2.2. 650–950 GHz receiving systems

The Nb–AlN–NbN junction technique [21,27,30] is used to implement much higher energy gaps (more than 3.15 mV even for junctions with high current density (Figure 3)) compared with traditional Nb–AlO_x–Nb and Nb–AlN–Nb structures with a gap of max. 2.8 mV [22,24]. High gap voltage provides substantial advantage due to the expanded bias voltage range where the SIS junction performs efficient signal mixing. For mixers set to signal receipt on frequencies from 700 to 1000 GHz, this is especially important because ... of the first Josephson step, that affects the mixer performance, falls into the quasi-particle step. This effect is demonstrated in Figure 4 on the dependences of the SIS mixer output power on bias voltage. At voltages about 1.5, 1.7 and 1.9 mV for the dashed, dotted and dashed-dotted lines, respectively, a negative peak occurs and is followed by rises on the right and on the left of the peak. Due to the presence of the peak with rises, an area with a width from 0.5 to 1 mV becomes unavailable to the mixer because the mixer gain in it can vary non-linearly depending on the signal power, and the stability of the whole mixer is deteriorated significantly due to the noise caused by the Josephson effect.

The shown singularities associated with the critical current manifestation are attributed to the difficulty of full suppression of the Josephson effect in the dual SIS junctions. It

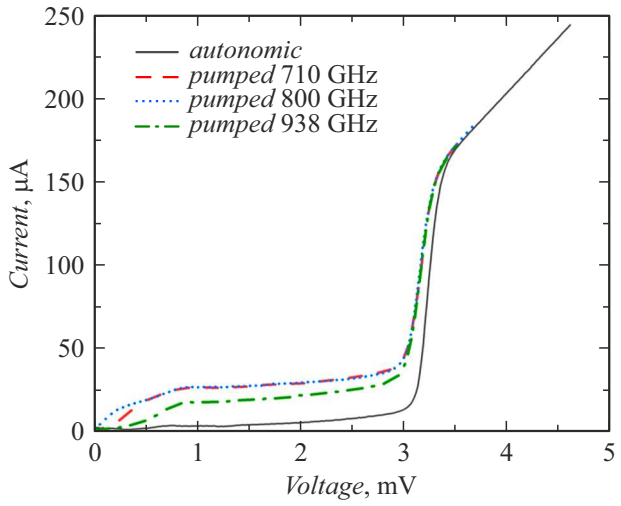

Figure 3. Nb–AlN–NbN SIS junction CVC. The solid curve shows the offline CVC with suppressed critical current. The other curves display CVC with optimum signal pumping by the reference-frequency oscillator with different frequencies: dashed line — 710 GHz, dotted line — 800 GHz, dashed and dotted line — 938 GHz.

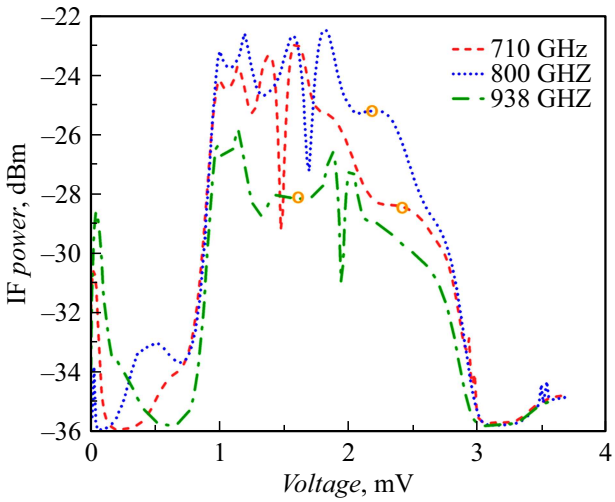

Figure 4. Measured curves showing the dependence of the SIS mixer intermediate-frequency output power on SIS junction voltage. The curves correspond to different frequencies of the reference oscillator: dashed line — 710 GHz, dotted line — 800 GHz, dashed-dotted line — 938 GHz. The IF power in integrated within 4–12 GHz. Circles on the curves show the bias voltages corresponding to the optimum operating point for the chosen reference oscillator frequency. During the measurement, the receiver input load was equivalent to the black body with 300 K.

is also important that the operating area contains the edge of exactly the first Josephson step that distorts CVC most heavily and, therefore, affects the differential resistance of the junction that defines matching between the junction and the intermediate frequency output path. Distortions corresponding to the peaks on curves in Figure 4 can be clearly seen on the SIS mixer response curves (Figure 5) that define its sensitivity. Thus, for example, the peak on the dotted line (reference oscillator frequency 800 GHz) located at 1.7 mV induces response distortions from 1.3 to 2.1 mV, therefore, the optimum operating point marked with a circle on the corresponding curve in Figure 4 falls onto 2.2 mV. In the operating point, the SIS mixer shall have the maximum response (Figure 5) and also a horizontal segment is extremely desirable in the operating point on the curves in Figure 4 because the mixer in this point will be most stable with respect to the output power level as long as the voltage noise will not be translated into the receiver output power level.

Figure 4 shows the operating points for the reference oscillator frequencies 710 GHz — 2.4 mV, 800 GHz — 2.2 mV, 938 GHz — 1.6 mV. The corresponding response defined as the receiver output power contrast for input loads of 77 and 300 K (so-called Y factor method) has the level of 1.8, 2.25, 1.4 dB (Figure 5). Note that for two lower frequencies of the reference oscillator, the operating point was located at a higher voltage than the problem area caused by the critical current, and on the highest frequency it shall be already below this area (Figure 4).

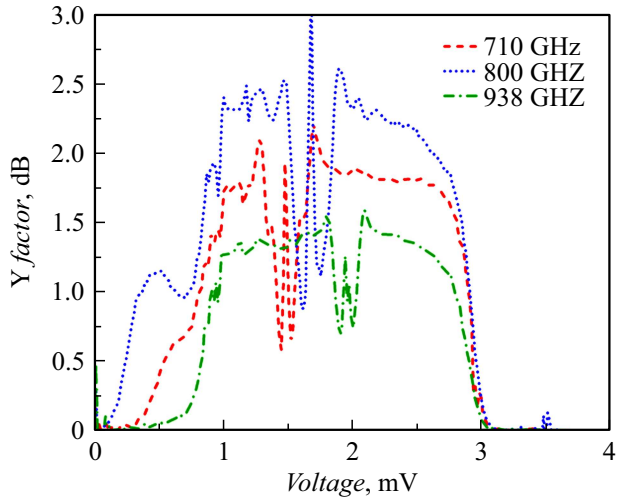

Figure 5. SIS mixer response measured by the Y factor method. Y factor is given in dB and is defined as the SIS output power ratio for loads of 300 and 77 K.

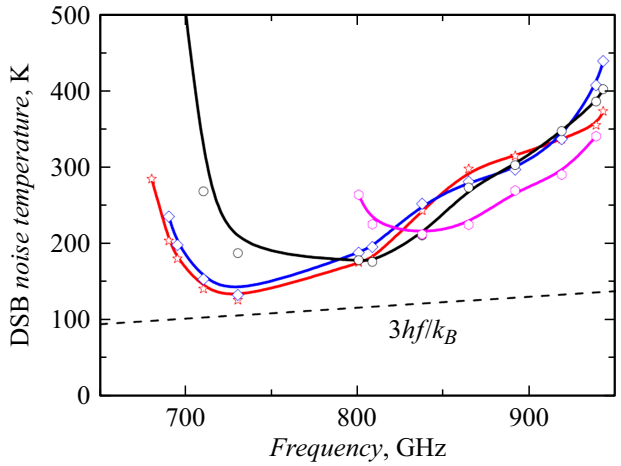

Figure 6. Noise temperature in the double-sideband (DSB) mode for four SIS mixers with different design depending on frequency. The dotted line shows the noise temperature corresponding to $3hf/k_B$.

This is because the best operating areas are most often located closer to the center of the quasi-particle step. Therefore, the Nb−AlN−NbN SIS junctions gap voltage of which is 0.35 mV as wide as for Nb−AlO_x−Nb technique provide a significant advantage. A series of investigations of waveguide SIS mixers has been conducted [21,29], the mixing element design has been improved. The noise temperature measurements in the double-sideband (DSB) mode for four SIS mixers with different design depending on frequency are sown in Figure 6. The dotted line shows the noise temperature corresponding to $3hf/k_B$ DSB.

Thus, the developed technique makes it possible to implement the tunneling current densities of the junctions up to 30 kA/cm^{2}with Rsg/Rn higher than 20. SIS mixers for the waveguide receiver with the operating frequency up to 950 GHz have been developed and tested [27]. The dual SIS junction design provides a wide operating range of the receiver (675 − 950 GHz) and quite good noise temperature in this range that can reach 120 K in the best points [21]. Mixers based on the dual Nb/AlN/NbN tunnel junctions included in the NbTiN/Al microstrip line [21,27] may be used for modernization of high-frequency 7-pixel matrix receivers for the CHAMP+ instrument installed on the APEX (Atacama Pathfinder EXperiment) telescope, input frequency range 790−950 GHz [31,32]. The developed SIS mixers may be also used for the Chinese observatory on the Dome A (Antarctic), for the Brazilian LLAMA telescope project in the Andes [33] and for the Millimetron space observatory (in a single telescope mode).

3. NbTiN film parameters

On higher frequencies, the hf photon energy exceeds the double energy of 2Δ Nb, and the transmission line electrode loss result in receiver performance deterioration [34]. Nb connections with higher energy gap (e.g. NbN and NbTiN) are used to overcome this frequency limit. To improve the methods of fabrication of integrated superconducting devices based on NbTiN films, the effect of various manufacturing processes on the quality and parameters of the fabricated structures has been studied. NbTiN films made in various conditions were examined using the TeraView TPS Spectra 3000 time-resolved THz spectrometer [35]. The measured transmittance spectra of the films on substrates are approximated by the multilayer media model expressions [36]. The superconducting properties are considered using the Zimmermann, model [37] that also considers the finite free path of quasiparticles.

Five types of experimental samples were prepared:

1) NbTiN film on Si substrate;

2) NbTiN film on the Al_2O_3 buffer layer deposited on the Si substrate;

3) NbTiN film on the Al_2O_3 buffer layer with anodized surface;

4) NbTiN film on the Al_2O_3 buffer layer with a thin Al layer on the surface;

5) NbTiN film on the Al_2O_3 buffer layer with a thin Al layer and anodized surface;

Film parametersΔ_0 — superconducting gap at $T = 0$ K, λ_0 — london penetration depth at $T = 0$ K, T_c — critical temperature and σ_0 — DC conductance in normal state near T_c for all test films are listed in the table. The temperature dependences Δ and λ for samples #2 and #5 are shown in Figure 7. It is shown that all additional layers have a minor effect on the film parameters. A small decrease in the critical temperature, gap and increase in the london penetration depth may be explained by the proximity effect between the NbTiN film and anodized Al layer.

Test film parameters

Sample No	d, nm	$\sigma_{0,DC}$, $10^4(\Omega \cdot cm)^{-1}$	$T_{c,DC}$ K	$\sigma_{0,TDS}$, $10^4\ (\Omega \cdot cm)^{-1}$	$T_{c,TDS}$, K	$2\Delta_0$, meV	λ_0, nm
#1	338	1.07	15.2	1.12	13.8	5.2	282
#2	330	1.03	15.1	1.09	13.9	5.0	283
#3	340	n.a.	n.a.	1.00	13.7	4.7	310
#4	340	n.a.	n.a.	1.07	13.8	4.8	295
#5	340	n.a.	n.a.	1.01	13.7	4.8	300

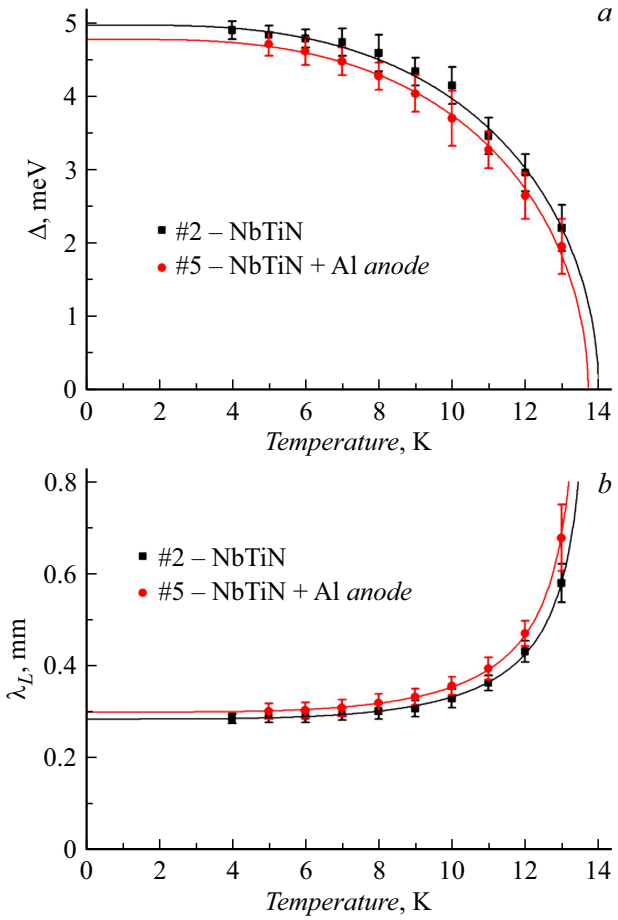

Figure 7. temperature dependences of the superconducting gap Δ (a) and london penetration depth (b) for samples #2 and #5.

Conclusions

We had designed, fabricated and tested a SIS mixer for a frequency range of 211−275 GHz. Non-corrected noise temperature equal to approx. 16.5 ± 2 K was measured on 255 GHz, which is only a little higher than the quantum value hf/k_B. This mixer meets the specifications of the „Millimetron“ space mission and may be used for new ground-based radio telescopes (Suffa, LLAMA). For high-frequency receivers, we used Nb−AlN−NbN mixers included in the NbTiN−Al microstrip line. Such mixers demonstrate DSB noise temperatures from 210 to 400 K and may be used for modernization of the 790−950 GHz high-frequency matrix receiver on the APEX telescope. The time-resolved terahertz spectrometry method was used to study the effect of various manufacturing processes on the quality and parameters of the fabricated NbTiN film structures

The study used Unique Research Facility „Kriointegral“ № 352529.

Funding

This study was supported by the Ministry of Science and Higher Education of the Russian Federation (Agreement № 075-15-2024-538). Development of the 800−950 GHz SIS mixer and fabrication technique was performed under the grant provided by RCF (№ 23-79-00019, https://rscf.ru/project/23-79-00019/). The 211−275 GHz SIS mixers were made and measured under the grant provided by RSF (№ 23-79-00061, https://rscf.ru/project/23-79-00061/)

Conflict of interest

The authors declare that they have no conflict of interest.

References

[1] J.R. Tucker, M.J. Feldman. Rev. Mod. Phys., **57**, 1055 (1985). DOI: 10.1103/RevModPhys.57.1055
[2] J. Zmuidzinas, P.L. Richards. Proc. IEEE, **92**, 1597 (2004). DOI: 10.1109/JPROC.2004.833670
[3] ALMA Observatory Website. Available online: https://www.almaobservatory.org/en/about-alma/
[4] Herschel Space Observatory Website. Available online: https://www.herschel.caltech.edu/
[5] E.L. Wolf, G.B. Arnold, M.A. Gurvitch, J.F. Zasadzinski. *Josephson Junctions. History, Devices, and Applications* (Jenny Stanford Publishing, NY., 2017), DOI: 10.1201/9781315364520
[6] J.R. Tucker. IEEE J. Quantum Electron., **15**, 1234 (1979). DOI: 10.1109/JQE.1979.1069931
[7] P.L. Richards, T.M. Shen, R.E. Harris, F.L. Lloyd. Appl. Phys. Lett., **34**, 345 (1979). DOI: 10.1063/1.90782
[8] A.R. Kerr, M.J. Feldman, S.-K. Pan. *Proceedings of the Eighth International Symposium on Space Terahertz Technology* (Cambridge, MA, USA, 25−27 March, 1997), p. 101.

[9] T. De Graauw, F.P. Helmich, T.G. Phillips, J. Stutzki, E. Caux, N.D. Whyborn, N. Trappe. Astronomy & Astrophysics, **518** (1), L6 (2010). DOI: 10.1051/0004-6361/201014698
[10] *First Image of a Black Hole Website*. Available online: https://eventhorizontelescope.org/press-release-april-10-2019-astronomers-capture-first-image-black-hole
[11] K. Akiyama, A. Alberdi, W. Alef, J.C. Algaba, R. Anantua, K. Asada, L.D. Matthews. Astronomy & Astrophysics, **681**, A79 (2024).
[12] *The Event Horizon Telescope Website*. Available online: https://eventhorizontelescope.org/
[13] *Millimetron Space Observatory Website*. Available online: http://millimetron.ru/index.php/en/
[14] I.D. Novikov, S.F. Likhachev, Yu.A .Shchekinov, A.S. Andrianov, A.M. Baryshev, A.I. Vasyunin, D.Z. Wiebe, Th. de Graauw, A.G. Doroshkevich, I.I. Zinchenko, N.S. Kardashev, V.I. Kostenko, T.I. Larchenkova, L.N. Likhacheva, A.O. Lyakhovets, D.I. Novikov, S.V. Pilipenko, A.F. Punanova, A.G. Rudnitsky, A.V. Smirnov, V.I. Shematovich. Phys. Usp., **64**, 386 (2021). DOI: 10.3367/UFNe.2020.12.038898
[15] T. Imamura, T. Shiota, S. Hasuo. IEEE Trans. Appl. Supercond., **2**, 1 (1992). DOI: 10.1109/77.124922
[16] T. Imamura, T. Shiota, S. Hasuo. IEEE Trans. Appl. Supercond., **2**, 84 (1992). DOI: 10.1109/77.139224
[17] M. Gurvitch, M.A. Washington, H.A. Huggins, Appl. Phys. Lett., **42**, 472 (1983). DOI: 10.1063/1.93974
[18] L.V. Filippenko, S.V. Shitov, P.N. Dmitriev, A.B. Ermakov, V.P. Koshelets, J.R. Gao. IEEE Trans. Appl. Supercond., **2001**, 816 (2001). DOI: 10.1109/77.919469
[19] A.A. Golubov, E.P. Houwman, J.G. Gijsbertsen, V.M. Krasnov, J. Flokstra, H. Rogalla, M.Yu. Kupriyanov. Phys. Rev. B, **51**, 1073 (1995). DOI: 10.1103/PhysRevB.51.1073
[20] P.N. Dmitriev, A.B. Ermakov, A.G. Kovalenko, V.P. Koshelets, N.N. Iosad, A.A. Golubov, M.Yu. Kupriyanov. IEEE Trans. Appl. Supercond., **9**, 3970 (1999). DOI: 10.1109/77.783897
[21] K.I. Rudakov, A.V. Khudchenko, L.V. Filippenko, M.E. Paramonov, R. Hesper, D.A. Lima, A.M. Baryshev, V.P. Koshelets. Appl. Sci., **11**, 10087 (2021). DOI: 10.3390/app112110087.
[22] A.W. Kleinsasser, R.E. Miller, W.H. Mallison, IEEE Trans. Appl. Supercond., **5**, 2318 (1995). DOI: 10.1109/77.403049
[23] J. Kawamura, D. Miller, J. Chen, J. Zmuidzinas, B. Bumble, H.G. LeDuc, J.A. Stern. Appl. Phys. Lett., **76**, 2119 (2000). DOI: 10.1063/1.126272
[24] B.D. Jackson, G. de Lange, T. Zijlstra, M. Kroug, T.M. Klapwijk, J.A. Stern. J. Appl. Phys., **97**, 113904 (2005). DOI: 10.1063/1.1927281
[25] B.D. Jackson, N.N. Iosad, G. De Lange, A.M. Baryshev, W.M. Laauwen, J.R. Gao, T.M. Klapwijk. IEEE Trans. Appl. Supercond., **11** (1), 653 (2001). DOI: 10.1109/77.919429
[26] J.W. Kooi, J.A. Stern, G. Chattopadhyay, H.G. LeDuc, B. Bumble, J. Zmuidzinas. Intern. J. Infrared Millimeter Waves, **19**, 373 (1998). DOI: 10.1023/A:1022595223782
[27] A. Khudchenko, A.M. Baryshev, K.I. Rudakov, P.M. Dmitriev, R. Hesper, L. de Jong, V.P. Koshelets. IEEE Trans. Terahertz Sci. Technol., **6**, 127 (2016). DOI: 10.1109/TTHZ.2015.2504783
[28] *UNU Kriointegral Website*. Available online: http://ckp-rf.ru/usu/352529/
[29] K.I. Rudakov. *Development of Advanced Superconductor-Insulator-Superconductor Mixers for Terahertz Radio Astronomy*, Ph.D. Thesis (University of Groningen, Groningen, The Netherlands, 2021), DOI: 10.33612/diss.174103493
[30] M.Yu. Torgashin, V.P. Koshelets, P.N. Dmitriev, A.B. Ermakov, L.V. Filippenko, P.A. Yagoubov, IEEE Trans. Appl. Supercond., 17, 379 (2007). DOI: 10.1109/TASC.2007.898624
[31] R. Güsten, R.S. Booth, C. Cesarsky, K.M. Menten, C. Agurto, M. Anciaux, F. Wyrowski. Proc. SPIE 6267, Ground-based and Airborne Telescopes, 626714 (2006). DOI: 10.1117/12.670798.
[32] C. Kasemann, R. Güsten, S. Heyminck, B. Klein, T. Klein, S.D. Philipp, A. Korn, G. Schneider, A. Henseler, A. Baryshev, T.M. Klapwijk. *Millimeter and Submillimeter Detectors and Instrumentation for Astronomy III*. Edited by J. Zmuidzinas, W.S. Holland, S. Withington, W. Duncan (Proceedings of the SPIE 6275, 62750N, 2006), DOI: 10.1117/12.670810
[33] *LLAMA Observatory Website*. Available online: https://www.llamaobservatory.org/
[34] D.C. Mattis, J. Bardeen. Phys. Rev., **111** (2), 412 (1958). DOI: 10.1103/PhysRev.111.412
[35] E.S. Zhukova, B.P. Gorshunov, L.S. Kadyrov, K.V. Zhivetev, A.V. Terentiev, A.M. Chekushkin, F.V. Khan, A.V. Khudchenko, N.V. Kinev, V.P. Koshelets. IEEE Trans. Appl. Supercond., **34** (3), 1100605 (2024). DOI: 10.1109/TASC.2024.3353139
[36] M. Born, E. Wolf. *Principles of Optics: Electromagnetic-Ttheory of Propagation, Interference and Diffraction of Light* (Pergamon Press, England, Oxford, 1987)
[37] W. Zimmermann, E.H. Brandt, M. Bauer, E. Seider, L. Genzel. Physica C: Superconduct., **183** (1-3), 99 (1991). DOI: 10.1016/0921-4534(91)90771-P

Translated by E.Ilinskaya